Predictable and precise porosity quantification in PBF-LB/M materials using automated optical microscopy

Maciej Tusz, Matthew Harris, Thomas Wendler

Angaben zur Veröffentlichung / Publication details:

Tusz, Maciej, Matthew Harris, and Thomas Wendler. 2026. "Predictable and precise porosity quantification in PBF-LB/M materials using automated optical microscopy." *Nano Micro Mechanics Review* 2 (1): 3–9. https://doi.org/10.1142/s3082805826400017.

ARTICLE

Nano Micro Mechanics Review

Predictable and precise porosity quantification in PBF-LB/M materials using automated optical microscopy

Maciej Tusz [*,†,¶], **Matthew Harris** [‡] **& Thomas Wendler** [*,§]

Highlights

- The Archimedes method for porosity estimation of PBF-LB/M materials results in a consistent overestimation in a sample set using copper alloys.
- A simple automated optical microscopy method is proposed that offers greater consistency and precision over Archimedes' density analysis.
- Our method exhibits a strong linear correlation between porosity and measurement variability (R^2 up to 0.92).

Graphical Abstract

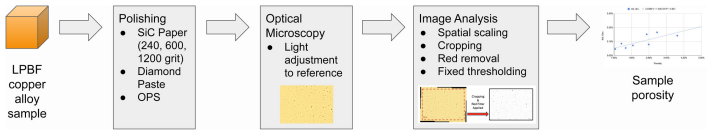

Abstract Accurate and objective porosity quantification is critical for Powder Bed Fusion-Laser Beam/Metal (PBF-LB/M) materials. This study compares the standardized Archimedes method against a simple automatic optical microscopy (OM) protocol for measuring porosity in copper alloy PBF-LB/M components. Across all trials, Archimedes reported porosity values atleast 1.3% higher than OM on paired samples and showed high, nonlinear measurement variability with mean porosity. In contrast, the OM protocol, utilizing rigorous sample preparation and a fixed-threshold analysis, provided superior consistency. OM results exhibited a strong linear correlation between measured porosity and measurement standard deviation (R^2 up to 0.92), demonstrating that its variability is structurally related to the actual porosity level. The proposed OM method offers a robust, predictable, and precise tool for R&D and quality control of additively manufactured components.

Keywords Porosity estimation; optical microscopy; metal additive manufacturing; metal laser powder bed fusion (LPBF); material characterization; copper.

1. Introduction

In the development of new materials for critical applications, such as those produced via Powder Bed Fusion-Laser Beam/Metal (PBF-LB/M), the need for robust, repeatable, and objective Quality Control (QC) tools is paramount 1. As operating environments and performance demands for advanced manufacturing materials intensify, the ability to accurately characterize structural integrity becomes a limiting factor in material adoption 2. Within Additive Manufacturing (AM), internal defects, specifically porosity, are the most critical flaw, severely degrading mechanical properties like fatigue life and ductility [3–5].

The quantitative measurement of porosity, however, is often subjective and highly variable depending on the measurement methodology employed and the operator performing the analysis [6, 7]. This inherent subjectivity hinders the ability to create reliable statistical process control (SPC) for advanced manufacturing processes like PBF-LB/M, where materials characterization is already expensive and time-consuming. To enable rapid R&D and QC necessary for the next generation of materials, methods must be developed that are more automated, objective, and repeatable.

Numerous approaches have been used to quantify porosity [6, 7]. The current standard for bulk density and porosity measurement is the

[*]Department of Diagnostic and Interventional Radiology and Neuroradiology, University Hospital Augsburg, Stenglinstr. 2, Augsburg 86156, Germany
[†]Magnitude Innovations Ltd., 8 Gainsborough Road, London E11 1HT, UK
[‡]AFU SAS, 64 Rue de la Ville ès Cours, Saint-Malo 35400, France
[§]Center for Advanced Analytics and Predictive Sciences, University of Augsburg, Universitätsstr. 2, Augsburg 86159, Germany
[¶]m.tusz@magnitude.am
[¶]Corresponding author.

Received 20 December 2025; Revised 3 February 2026; Accepted 27 February 2026; Published 15 May 2026; doi:10.1142/S3082805826400017

Archimedes method (e.g. ISO 3369). This buoyancy-based technique is simple to implement but measures only the total volumetric porosity, offering no insight into pore morphology (size, shape, or distribution). Its primary weakness is its susceptibility to systematic error, including incomplete saturation of surface-connected pores and operator variability during surface preparation and measurement [7]. These limitations result in porosity measurements that can be inconsistent and inaccurate, especially in low-porosity, high-density AM applications.

Alternatively, more advanced methods include X-ray Computed Tomography (CT) and Optical Microscopy (OM) [8]. CT provides comprehensive, non-destructive three-dimensional pore characterization, which is ideal for research but typically too slow and expensive for high-throughput R&D or routine QC [9−11]. OM, conversely, is cost-effective and provides high-resolution two-dimensional data. However, OM's reliability relies heavily on rigorous, systematic sample preparation and complex image analysis protocols to ensure that the 2D cross-section accurately represents the bulk material [6, 12].

To address the critical gap in needing a robust, cost-effective, and precise method for rapid porosity quantification in PBF-LB/M materials, this paper proposes a simple automatic OM analysis protocol [7]. The central objective of this study is to directly validate this novel optical porosity analysis approach for repeatability and objectively accurate results by comparing its performance against the standardized Archimedes method. We specifically analyze measurement consistency and variability across a range of porosities. We hypothesize that the systematic OM method will demonstrate superior consistency, a predictable linear correlation between measurement variability and actual porosity level, and overall higher precision than the Archimedes method, thereby providing a more reliable tool for R&D and QC of high-performance metal components.

2. Methods

To evaluate the proposed approach of porosity analysis, copper alloy samples fabricated with PBF-LB/M were evaluated under the standardized Archimedes approach and compared with the proposed optical method.

2.1. Sample manufacture

Samples were manufactured on an EOS M290 400W (EOS GmbH, Krailling, Germany) PBF-LB/M system at AFU in France. The copper powder and parameters were varying and proprietary; the primary goal was to arrive at various porosity values in order to evaluate and compare the Archimedes and OM approaches. Two batches of samples were produced, one with moderate porosity in Trials 1 and 2, and two with minimal porosities in Trials 3 and 4.

The samples manufactured were all 10 mm density cubes built in a diagonal across the build area in order to avoid regions of the build that are known to have process instabilities, as well as avoid interaction of the laser, smoke, and recoater during manufacture. The samples were exposed in a diagonal fashion, every layer from the front left to the back right.

2.2. Archimedes' analysis

Archimedes was measured on a Mettler Toledo ME204T/00 analog scale (Columbus, OH, USA) with a density measurement kit according to ISO 3369. The samples are weighed in air on the open pan, then immersed in deionized water with a wetting agent. If any bubbles appear on the surface, the sample is agitated to remove them. Each sample was measured three times to compute the mean porosity and standard deviation.

2.3. Optical microscopy analysis

OM samples were prepared following the same procedure to eliminate operator variability. All samples were first polished in three stages with Silicon Carbide paper. The first polish was performed with 240-grit paper, at a speed of 150 rpm and force of 25 Newtons for 1 min. Subsequent polishing was done with 600 and 1200 grit paper with the same speed, force, and duration. Finally, the samples were polished with a 3 μm diamond paste at a speed of 150 rpm and force of 25 Newtons for 3 min, and then a 0.04 μm oxide polishing suspension (OPS) at a speed of 150 rpm and force of 15 Newtons for 1 min. Table 1 summarizes the steps.

Imaging was performed with a single optical microscope, the Olympus GX53 (Olympus, Tokyo, Japan), with a motorized stage at 10x. The images consisted of 9 images that were stitched together with the help of the Olympus Stream software. Light intensity was calibrated based on a reference sample with established initial porosity before continuing to the subsequent samples in order to ensure repeatability. The image dynamic range was 8-bit.

For the OM analysis, ImageJ version 1.54 r (Wayne Rasband and contributors, National Institutes of Health, USA) was used as the image processing tool. All samples were taken with a calibration scale in the images. The resulting calibration was 270 pixels = 200 μm. From each image that was stitched from 9 10x images, the images were cropped in an automated way to ensure that the area of focus is consistent across all images, namely, cropping the borders by 150 pixels on every side to create a final image of 3656 × 2712 pixels (Fig. 1(a)). Because this is a copper alloy, the images were preprocessed by removing the red channel and averaging the green and blue channels to enhance pore contrast (Fig. 1(b)). Since no etching was performed on the samples, any visible artifacts at this point were assumed to be pores in the samples.

We evaluated two approaches to determine porosity. First, we

Table 1. Sample preparation steps for OM analysis.

Polishing step	Medium	Abrasive size	Speed	Force	Duration
1	SiC paper	240 grit	150 rpm	25 N	1 min
2	SiC paper	600 grit	150 rpm	25 N	1 min
3	SiC paper	1200 grit	150 rpm	25 N	1 min
4	Diamond paste	3 μm	150 rpm	25 N	3 min
5	OPS	0.04 μm	150 rpm	15 N	1 min

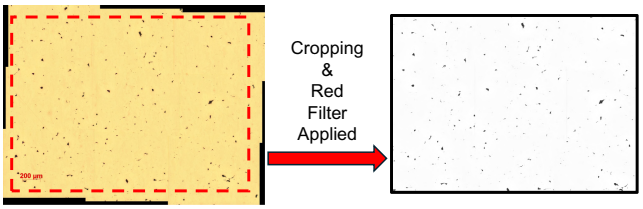

Fig. 1. (a) Preprocessing of stitched images, consisting of cropping the borders (left) and (b) removing the red channel and averaging the green and blue in a grayscale image (right).

utilized the Otsu thresholding method [13], an automated algorithm that determines an optimal threshold by minimizing intra-class variance in the image histogram, to determine the areas of porosity, and then evaluated fixed thresholds. We then established a testing protocol to see the variability of porosity based on a fixed thresholding range of between 155 and 170 out of 255, based on 8 bit dynamic range, i.e. 60.7−66.7%. Finally, artifacts that had a maximum Feret diameter of less than 5 μm were removed from the analysis as they are primarily attributed to noise in the thresholding [11].

No accepted standard exists for porosity measurements of metallic samples; we propose the following systematic method. First, a reference sample was established that was utilized for any subsequent measurements with the help of a relative scale. Next, the sample was quantified, and after the results agreed with established values, subsequent samples were imaged. This ensured that lighting and any other possible operator variations were consistent throughout image capture (Fig. 2).

To minimize variability, we first quantified the porosity of the reference sample at a threshold of 160 and then kept this reference sample to ensure repeatability of optical settings going forward.

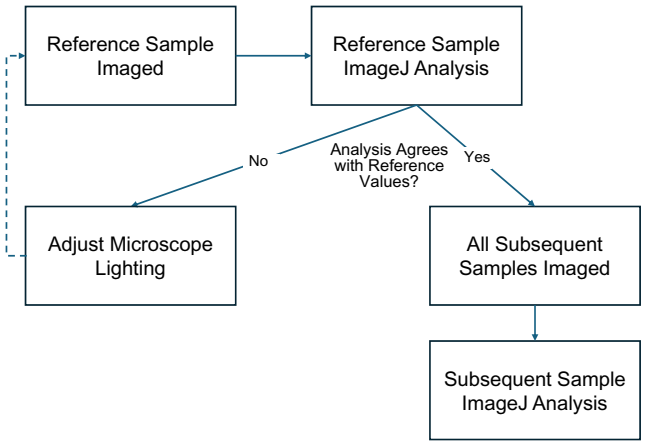

Fig. 2. Systematic method for reference sample calibration and optical porosity imaging.

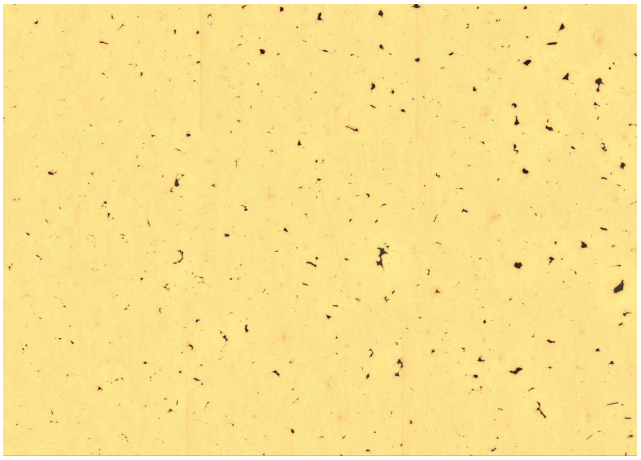

Fig. 3. Reference sample for imaging analysis exhibiting a consistent porosity distribution and high measurement variability for accurate imaging calibration, %A = 0.525, Count = 230. Image courtesy of AFU.

Because we did not have a statistical amount of measurements completed on the reference sample, we utilized the following values from analysis as our acceptance criteria before continuing imaging of further samples: %Area of 0.525 ± 5% and Count of 230 ± 5%. The sample chosen for this reference standard had a good balance of porosity and one of the highest standard deviations across varying thresholds of 0.020%, thus being a suitable candidate as a reference sample, as shown in Fig. 3.

The samples were then imaged across any given trials and analyzed with ImageJ through a batch process across thresholds of 155, 160, 165, and 170. These results were then averaged to determine an average porosity value as well as the standard deviation, in effect simulating imaging variations.

3. Results

3.1. Archimedes trials

For the Archimedes analysis, three measurements per sample were performed to ensure statistical significance of the porosity/density results. A reference value for density of 8.9 g/cm^3 was used to determine porosity values. For all porosity measurements, standard deviations of the porosity were calculated and plotted against the porosity values for Trials 1−4 as shown in Figs. 4(a)−4(d), respectively. The range of porosity for Trials 1 and 2 ranged between 2.15% and 4.32 % for Trials 1 and 2 (average 3.14%), while for Trials 3 and 4, the range was 1.45% to 3.91% (average 2.18%).

For all the Archimedes trials, results appear to show porosity of at least 1.3%. Additionally, the standard deviation of the results for all the trials shows a significant amount of nonlinear variability. There is no linear correlation between part porosity and the measurement standard deviation, as seen by R^2 correlations of 0.075, 0.515, 0.165, and 0.104. Moreover, the slope between average porosity and standard deviation was negative in all but one trial (Trial 3).

3.2. Optical imaging trials

Based on the automated thresholding of nearly all the images that were utilized for the analysis, the Otsu method determined that a good thresholding value lies in the range of 145−180 (Fig. 5(a)) for the 8-bit dynamic range of the images. When the sample contained fewer artifacts, it was observed that the automated Otsu thresholding median values were skewed and resulted in negligible thresholds that would lead to imaging errors (Fig. 5(b)) [12]. As a result, the fixed threshold approach detailed above was used subsequently.

Using the fixed threshold method proposed above, the porosity range for Trials 1 and 2 ranged between 1.05% and 4.50% for Trials 1 and 2 (average 2.57%), while for Trials 3 and 4, the range was 0.02% to 1.09% (average 0.27%). Based on these results, the methods yielded significantly different porosity estimates (paired Wilcoxon signed-rank test, $p = 5.6 \times 10^{-10}$).

Just like with Archimedes' trials, standard deviations for optical imaging were calculated, this time across the threshold ranges from 155 to 170. These values were plotted against the porosity measurements for trials 1−4 in Figs. 6(a)−6(d), respectively.

For optical imaging, it was found that the sample measurements had a linear correlation between total porosity and their measurement standard deviation. This linear relationship led to R^2 values of 0.621, 0.560, 0.763, and 0.920 for Trials 1−4, respectively. The linearity of these results suggests that there is a direct correlation between overall porosity and measurement accuracy, with lower porosity samples lending themselves to less variability in

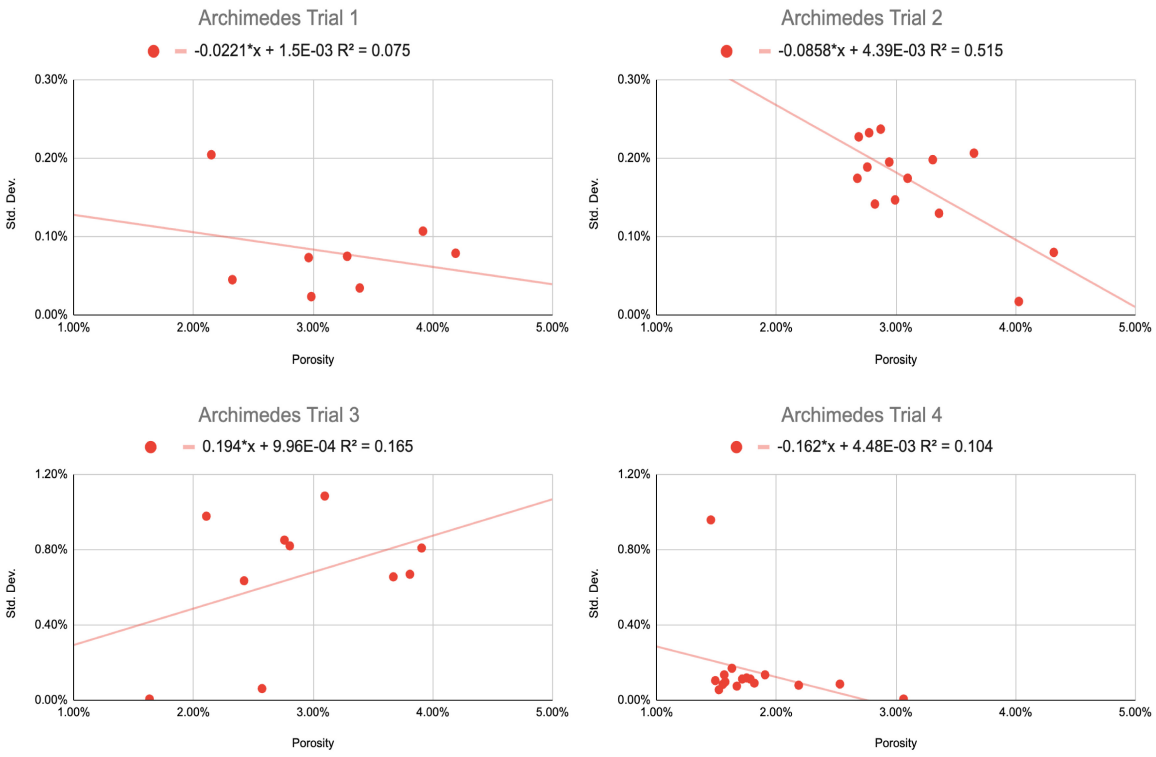

Fig. 4. Archimedes results for all trials. Note the standard deviation range in the charts for trials 1 and 2 is 0−0.3% while for trials 3 and 4 it is 0−1.2% — these ranges were selected for best visualization.

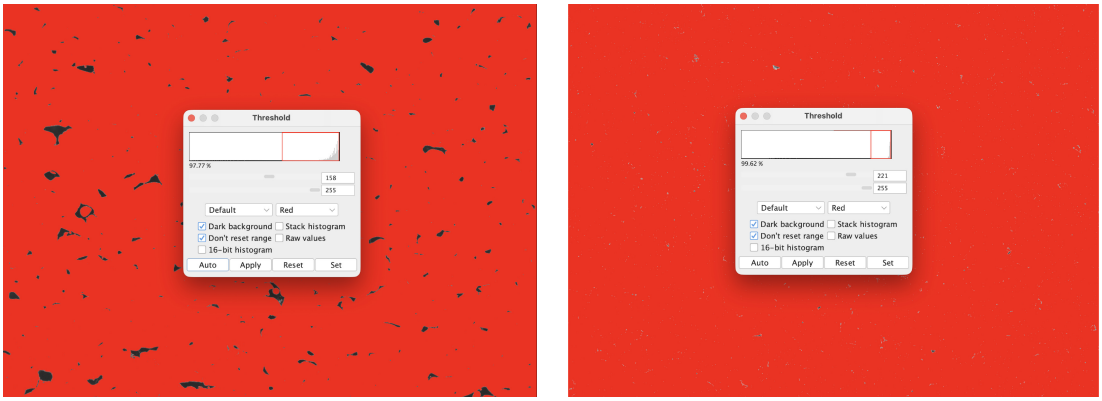

(a) Acceptable Thresholding (b) Extreme Thresholding

Fig. 5. Otsu thresholding using ImageJ.

measurements. Linear fit showed positive slopes for all Trials in the same order of magnitude, namely 0.0214 to 0.0386 and intercepts close to zero.

The linear correlation equations as well as R^2 correlations are summarized in Table 2 for all Archimedes and Optical Imaging Trials.

4. Discussion

The results of this study demonstrate a significant difference in porosity measurement when comparing the standardized Archimedes method to the proposed OM analysis, particularly concerning consistency and measurement variability.

4.1. Comparison of measurement techniques

The Archimedes analysis consistently reported a porosity of at least 1.3% for all trials, even in batches expected to have minimal porosity (0−1% based on optical analysis in Trials 3 and 4). Furthermore, the Archimedes standard deviation plots (Fig. 4) showed a high degree of nonlinear variability across all trials, with very low to moderate coefficients of determination (R^2 from 0.075 up to 0.515). This lack of correlation between the measured porosity and its measurement variability indicates that the Archimedes method introduces a random error independent of the actual porosity level. Finally, the Archimedes trials exhibited variability of measurement that was

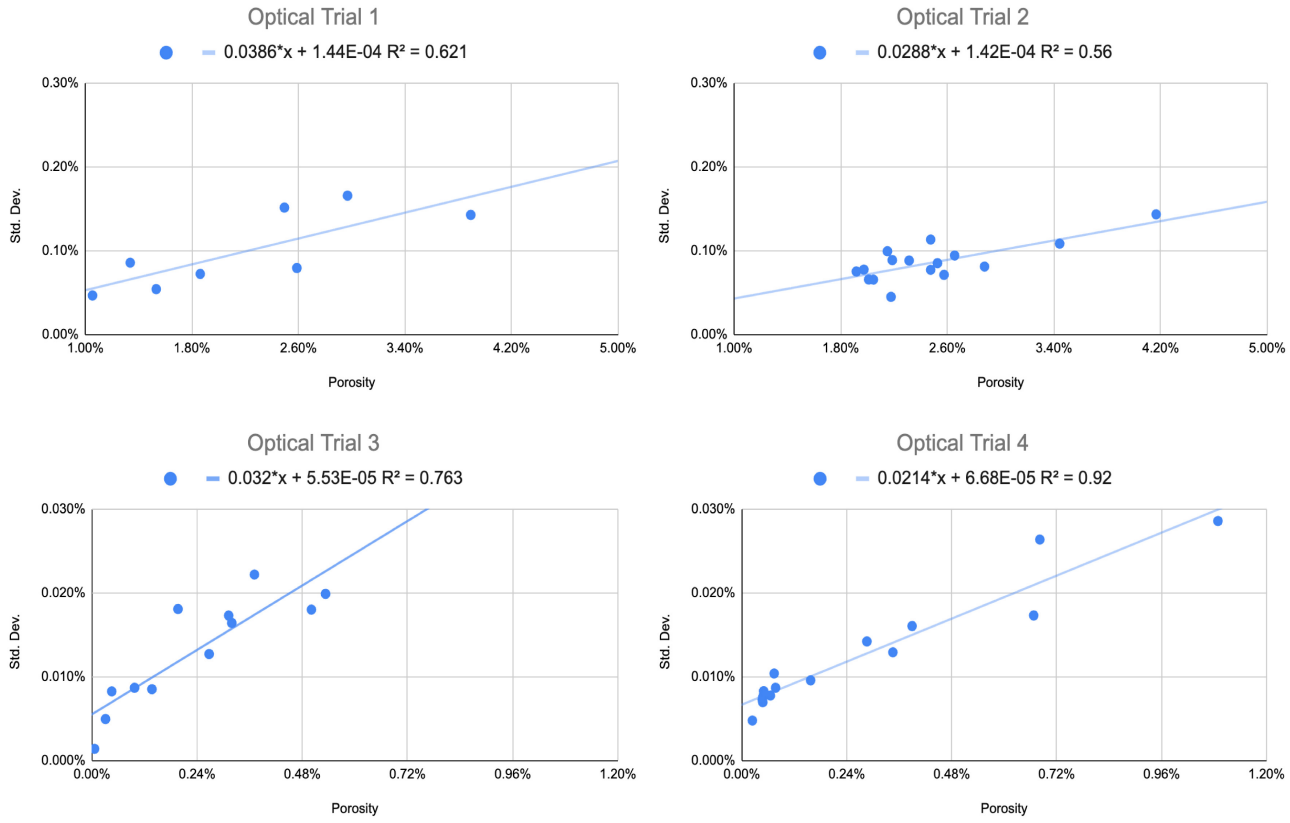

Fig. 6. Optical trials focusing on higher porosity samples (a) top-left, (b) top-right, and lower porosity samples (c) bottom-left and (d) bottom-right. Note that the scale of standard deviation for Trials 1 and 2 is 0–0.3% and porosity range of 1–5% while the standard deviation scale of Trials 3 and 4 is 0–0.03% and porosity is 0–1.2% — these ranges were selected for best visualization.

Table 2. Linear fit and coefficient of determination for Archimedes and optical trials.

Measurement type	Trial #	Linear fit equation	Coefficient of determination (R^2)
Archimedes	1	−0.0221x + 0.0015	0.075
Archimedes	2	−0.0858x + 0.0044	0.515
Archimedes	3	0.1940x + 0.0010	0.165
Archimedes	4	−0.1620x + 0.0045	0.104
Optical	1	0.0386x + 0.0001	0.621
Optical	2	0.0288x + 0.0001	0.560
Optical	3	0.0320x + 0.0000	0.763
Optical	4	0.0214x + 0.0001	0.920

inconsistently decreasing with porosity, like in Trials 1, 2, and 4 (negative slope of fitted line) — an implausible physical relationship.

Upon first analysis of Trials 1 and 2, this could possibly be due to the surface-connected pore nature of the samples and the fact that the ISO 3369 standard was used to measure density, which is not the most conducive to surface-connected materials. However, this is negated by the fact that Trials 3 and 4 had very little porosity, and hence very few surface-connected pores, yet exhibited even lower coefficients of determination of 0.165 and 0.104. The second source of measurement variability is potentially the fact that PBF-LB/M fabricated parts are never exactly the dimensions that are intended due to the nature of the process, specifically with regard to beam offset and part warpage due to the exposure of the layers, which are geometry dependent. Therefore, even though the cubes were designed with straight walls in mind, these walls tend to look wavy upon closer inspection, leading to a different volume than initially intended. However, this would result in a consistent offset that is exemplified by the 1.3% offset from the optical results for all the samples, while the measurement accuracy would not be affected, as is the case.

In contrast, the OM analysis yielded a strong linear correlation between the measured total porosity and the measurement standard deviation for all trials. R^2 values ranged from 0.56 to 0.92, while the slopes for each trial varied between 0.0214 and 0.0386, with the intercepts almost zero. This linearity suggests that the variability in the optical measurements is directly proportional to the amount of porosity present in the sample. Specifically, lower porosity samples (Trials 3 and 4) exhibited significantly lower measurement standard deviations compared to higher porosity samples (Trials 1 and 2), confirming that the method's accuracy increases as the porosity decreases. The strong linear fit for the optical trials, as summarized in Table 2, offers a predictable relationship for understanding measurement error that can be utilized to correct measurements and correlate trials across a wide range of porosity values with each other.

Furthermore, the OM approach provides invaluable insights into the pore shapes, distributions (aspects not presented here), and hence, process stability during manufacture without any additional effort or testing [14]. This information can thus be further used to

quantify the porosity and material properties and drive insights into how to improve and qualify the process for production readiness.

4.2. Methodological considerations and error sources

The observed systematic overestimation by the Archimedes method is likely attributable to the inherent difficulty of ensuring complete saturation and preventing micro-bubble formation on the sample surface, even with the use of a wetting agent and agitation, as outlined in the methods.

To exclude these possible sources of error from the Archimedes method, future work should focus on comparing these results with either ISO 2738 or ASTM B962, both of which are intended to determine material density for materials with surface-connected pores. Also, it would be important to compare these results with the standard measurement error for the used measurement system as well as for the ISO 3369 standard itself. Unfortunately, when it comes to the PBF-LB/M samples themselves, there is not much that can be done to correct the dimensional accuracy of the cubes, except to potentially manufacture near net-shape components and machine the final cube dimensions utilizing wire electrical-discharge machining (wire EDM) in order to avoid cold-working the material and favorably deforming the parts on the worked surfaces, as observed through other processes like shot-peening.

Otsu thresholding is an automated process that classifies pixels from the image's histogram into two classes separated by a threshold value t and then minimizes the variance within the classes or maximizes the mean between the classes [13]. This method is problematic in our analysis when there is noise in the form of small artifacts, more than two unique peaks in the histogram, or there is a light gradient across the sample. In such cases, the Otsu thresholding results in skewed values, as in our trial for samples with very low porosity. The problem of a non-binary distribution or the means being too close between the classes requires a threshold that is selected for the target application and then consistently applied.

For the optical imaging method, the key to its greater consistency and correlation lies in the rigorous sample preparation and systematic imaging protocol. The standardized polishing procedure (Table 1) minimized surface artifacts, and the use of a reference sample for light calibration (Fig. 2) ensured repeatability across image capture. The finding that automated Otsu thresholding was skewed for low-porosity samples (Fig. 5(b)) justified the subsequent use of a fixed, averaged threshold range (155−170 for 8-bit, i.e. 60.7−66.7% of the dynamic range) across all samples, reducing the reliance on a potentially unreliable automated algorithm when few artifacts (pores) were present. The strong linear correlation between porosity and standard deviation in the optical method suggests that the main source of variability stems from the actual structural heterogeneity of the pores being sampled, and not from the measurement process itself.

Additionally, the optical imaging approach demonstrates that constraining the sample preparation is effective in normalizing measurement bias and needs to be investigated further. Although variations in porosity were induced through varying thresholding of the images, this should be repeated by changing physical parameters in a controlled environment, such as varying light intensity of the OM or varying the sample preparation methods, to determine if a more robust method with reduced variability is possible.

5. Conclusions

While the Archimedes method is standardized, its application here demonstrates a lack of sensitivity and precision necessary for characterizing low-porosity additively-manufactured components as necessary for R&D and QC purposes. The measurement variability in Archimedes is nonlinear and unrelated to the actual porosity, suggesting a significant random operational error, again confirming that the variability in porosity measurements is independent of the porosity volume fraction, as would be expected.

The OM analysis, however, proved to be a more precise and consistent method for quantifying porosity in these samples. The rigorous sample preparation and systematic imaging protocol successfully minimized operator-induced variability. Unlike the Archimedes results, the optical method demonstrated a strong, predictable linear relationship between the measured porosity and the measurement standard deviation (R^2 up to 0.92). This consistency indicates that the method's variability is primarily structural — related to the actual amount of porosity — and offers a robust foundation for R&D and QC of additively-manufactured components.

Competing Interests

The authors declare that no competing interests related to the work presented here exist.

ORCID

Maciej Tusz https://orcid.org/0009-0004-5430-6248
Matthew Harris https://orcid.org/0009-0006-4269-2959
Thomas Wendler https://orcid.org/0000-0002-0915-0510

References

[1] A. Engelhardt, T. Wegener and T. Niendorf. A pragmatic approach for rapid, non-destructive assessment of defect types in laser powder bed fusion based on melt pool monitoring data. *Materials* **17**(13), p. 3287, 2024, doi: 10.3390/ma17133287.
[2] H. Liu *et al.*, Review on fatigue of additive manufactured metallic alloys: Microstructure, performance, enhancement, and assessment methods. *Advanced Materials* **36**(17), p. 2306570, 2024, doi: 10.1002/adma.202306570.
[3] P. D. Nezhadfar, S. Thompson, A. Saharan, N. Phan and N. Shamsaei. Structural integrity of additively manufactured aluminum alloys: Effects of build orientation on microstructure, porosity, and fatigue behavior. *Additive Manufacturing* **47**, p. 102292, 2021, doi: 10.1016/j.addma.2021.102292.
[4] C. Ye, C. Zhang, J. Zhao and Y. Dong. Effects of post-processing on the surface finish, porosity, residual stresses, and fatigue performance of additive manufactured metals: A review. *Journal of Materials Engineering and Performance* **30**(9), pp. 6407−6425, 2021, doi: 10.1007/s11665-021-06021-7.
[5] C. Du *et al.*, Pore defects in laser powder bed fusion: Formation mechanism, control method, and perspectives. *Journal of Alloys and Compounds* **944**, p. 169215, 2023, doi: 10.1016/j.jallcom.2023.169215.
[6] D. Wang *et al.*, A review and a statistical analysis of porosity in metals additively manufactured by laser powder bed fusion. *Opto-Electronic Advances* **5**(10), pp. 210058−1, 2022, doi: 10.29026/oea.2022.210058.
[7] E. Westphal and H. Seitz. Porosity and density measurement of additively manufactured components: A comparative analysis of measurement methods across processes and materials. *Materials Science in Additive Manufacturing* **4**(2), p. 025090010, 2025, doi: 10.36922/MSAM025090010.
[8] J. Wilbig, A. E. Wilson-Heid, L. Bernard, J. Baptista and A.-F. Obaton. Comparison of porosity analysis based on X-ray computed tomography on metal parts produced by additive manufacturing. *Applied Sciences* **15**(18), p. 9876, 2025, doi: 10.3390/app15189876.
[9] A. Thompson, I. Maskery and R. K. Leach. X-ray computed tomography for additive manufacturing: A review. *Measurement Science and Technology* **27**(7), p. 072001, 2016, doi: 10.1088/0957-0233/27/7/072001.
[10] A. du Plessis, I. Yadroitsev, I. Yadroitsava and S. G. Le Roux. X-ray micro-computed tomography in additive manufacturing: A review of the current

technology and applications. *3D Printing and Additive Manufacturing* **5**(3), pp. 227–247, 2018, doi: 10.1089/3dp.2018.0060.

[11] V. A. J. Jaques *et al.*, Review of porosity uncertainty estimation methods in computed tomography dataset. *Measurement Science and Technology* **32**(12), p. 122001, 2021, doi: 10.1088/1361-6501/ac1b40.

[12] T. Yang *et al.*, A review of diagnostics methodologies for metal additive manufacturing processes and products. *Materials* **14**(17), p. 4929, 2021, doi: 10.3390/ma14174929.

[13] N. Otsu. A threshold selection method from gray-level histograms. *IEEE Transactions on Systems, Man, and Cybernetics* **9**(1), pp. 62–66, 1979, doi: 10.1109/TSMC.1979.4310076.

[14] S. Ball, M. Ghayoor, S. Pasebani and A. Tabei. Statistical analysis of porosity and process parameter relationships in metal additive manufacturing. *Procedia Manufacturing* **53**, pp. 343–347, 2021, doi: 10.1016/j.promfg.2021.06.037.